Am J Nucl Med Mol Imaging 2021;11(5):415-427
www.ajnmmi.us /ISSN:2160-8407/ajnmmi0135122

Original Article

Implementation of FDG-PET/CT imaging methodology for quantification of inflammatory response in patients with locally advanced non-small cell lung cancer: results from the ACRIN 6668/RTOG 0235 trial

Pegah Jahangiri[1*], Alexandra D Dreyfuss[1*], Fenghai Duan[2], Bradley S Snyder[3], Austin J Borja[1], Kamyar Pournazari[1], Esha Kothekar[1], Leila Arani[1], Abdullah Al-Zaghal[1], Siavash Mehdizadeh Seraj[1], Emily C Hancin[1], Benjamin Pinheiro[1], Thomas J Werner[1], Samuel Swisher-McClure[4], Steven J Feigenberg[4], Drew A Torigian[1], Mona-Elisabeth Revheim[1,5,6], Charles B Simone II[7], Abass Alavi[1]

[1]Department of Radiology, Hospital of The University of Pennsylvania, Philadelphia 19104, PA, USA; [2]Department of Biostatistics and Center for Statistical Sciences, Brown University School of Public Health, Providence 02912, RI, USA; [3]Center for Statistical Sciences, Brown University School of Public Health, Providence 02912, RI, USA; [4]Department of Radiation Oncology, Hospital of The University of Pennsylvania, Philadelphia 19104, PA, USA; [5]Division of Radiology and Nuclear Medicine, Oslo University Hospital, Oslo 0424, Norway; [6]Institute of Clinical Medicine, Faculty of Medicine, University of Oslo, Oslo 0424, Norway; [7]Department of Radiation Oncology, New York Proton Center, New York 10035, NY, USA. [*]Co-first authors.

Received May 10, 2021; Accepted August 8, 2021; Epub October 15, 2021; Published October 30, 2021

Abstract: We measured changes in 18F-fluorodeoxyglucose (FDG) uptake on positron emission tomography/computed tomography (PET/CT) images in the lung parenchyma to quantify the degree of lung inflammation in patients with locally advanced non-small cell lung cancer (NSCLC) who received radiotherapy (RT). The goal of this study was to demonstrate successful implementation of this imaging methodology on NSCLC patients and to report quantitative statistics between pre-RT and post-RT. Seventy-one patients with NSCLC underwent FDG-PET/CT imaging before and after RT in a prospective study (ACRIN 6668/RTOG 0235). Comparisons between pre-RT and post-RT PET/CT were conducted for partial volume corrected (PVC)-mean standardized uptake value (SUVmean), PVC-global lung parenchymal glycolysis (GLPG), and lung volume for both ipsilateral and contralateral lungs using the nonparametric Wilcoxon signed-rank test. Regression modeling was conducted to associate clinical characteristics with post-RT PET/CT parameters. There was a significant increase in average SUVmean and GLPG of the ipsilateral lung (relative change 40% and 20%) between pre-RT and post-RT PET/CT scans ($P<0.0001$ and $P=0.004$). Absolute increases in PVC-SUVmean and PVC-GLPG were more pronounced (ΔPVC-SUVmean 0.32 versus ΔSUVmean 0.28; ΔPVC-GLPG 463.34 cc versus ΔGLPG 352.90 cc) and highly significant ($P<0.0001$). In contrast, the contralateral lung demonstrated no significant difference between pre-RT to post-RT in either GLPG ($P=0.12$) or SUVmean ($P=0.18$). The only clinical feature significantly associated with post-RT PET/CT parameters was clinical staging. Our study demonstrated inflammatory response in the ipsilateral lung of NSCLC patients treated with photon RT, suggesting that PET/CT parameters may serve as biomarkers for radiation pneumonitis (RP).

Keywords: FDG-PET/CT, radiotherapy, radiation pneumonitis, lung cancer

Introduction

Lung cancer is the leading cause of cancer death worldwide, with one of the lowest 5-year survival rates (18%) among all cancers [1]. According to projections from the American Cancer Society, there will be an estimated 228,820 new incidences of lung cancer by the end of 2020, and an estimated 135,720 people will die from lung cancer by the end of the same year. Non-small cell lung cancers (NSCLC), including squamous cell carcinoma, adenocarcinoma, and large cell carcinoma, represent 85% of lung malignancies, and an estimated US incidence of over 180,000 [2, 3]. Despite advances in treatment, overall survival remains

poor, owing partly to the difficulty in detecting early stage disease; only 10% of patients with Stage IVA-B disease survive beyond 60 months [4]. The standard of care for treating patients with locally advanced NSCLC combines chemotherapy and radiotherapy, delivered concurrently, followed by one year of immunotherapy [5].

Radiation therapy (RT) has been the mainstay of treatment by achieving local control of disease, with approximately 50% of all patients with solid malignant tumors expected to receive RT at some point in their disease course [5]. RT utilizes ionizing radiation to destroy tumor cells via DNA and cellular damage, and it is therefore contingent upon the selective targeting of abnormal tumor cells and the sparing of normal tissue. However, despite the many technological advancements that have revolutionized RT, dose delivery to surrounding normal tissue is often unavoidable and can result in significant toxicities that may impair quality of life and survival [6-8].

For lung cancer patients receiving definitive chemoradiation, radiation-induced pneumonitis (RP) is one of the most commonly manifested complications, and it is estimated to occur in up to 50% of patients [5, 9-11]. A multifactorial process mediated by a cascade of inflammatory cytokines that cause nonspecific symptoms (such as cough, dyspnea, and respiratory failure) anywhere from several weeks to 1-year post-RT, RP represents a major clinical challenge [12, 13]. Because RP can result in significant mortality and morbidity, it may significantly impact patients' quality of life and post-RT outlook, even if their treatments are successful in achieving remission. Current clinical strategies for the management of RP are limited, relying primarily on functional lung testing and anatomical imaging for diagnosis and corticosteroids as the main treatment method [14]. Computed tomography (CT) remains the most commonly used imaging technique in the evaluation of patients' response to treatment, as well as for the diagnosis of RP in NSCLC [14, 15]. However, an anatomically-based CT evaluation can yield misleading results as the method is generally insensitive to biological changes appearing much earlier than structural alterations [15]. Functional and molecular imaging with novel positron emission tomography (PET) and magnetic resonance imaging (MRI) techniques give a more detailed insight into the molecular mechanisms and quantitation of response than does anatomical imaging alone [16]. Although corticosteroids are effective in the acute exudative phase of injury, they have minimal effect after fibrosis has developed [17, 18]. As patients who are diagnosed early and promptly treated with steroids have a superior overall prognosis, it is therefore imperative to detect RP at an early stage [19].

Recently, a number of studies have reported patient- and treatment-related factors associated with increased risk of RP, such as delivered radiation dose and volume irradiated [20, 21]. For example, one meta-analysis reported age over 65 years, dosimetric lung volume (i.e. uninvolved total lung) receiving ≥20 Gy (V20), and concurrent chemoradiotherapy (CCRT) schemes as predictive factors for RP [22]. However, other studies have reported no associations between age and RP [23-25], and there is currently no established method to predict the onset and/or development of RP [26]. Thus, potential RP patients would benefit greatly from a post-therapy method for the early diagnosis of adverse events [27].

One promising approach involves the use of molecular imaging techniques to gain insight into RP at the molecular level. In recent years, 18F-2-fluoro-2-deoxy-D-glucose (FDG)-PET/CT has emerged as a powerful tool to assess the extent of pulmonary inflammation after thoracic RT, characterized by increased FDG uptake in the lung parenchyma. After FDG, an analog of glucose, is taken up by the cell, it is phosphorylated by hexokinase and trapped within the cell, unable to proceed through glycolysis. Consequently, FDG uptake is the result of high glucose utilization by infiltrating inflammatory cells present in neoplastic disorders [21, 28, 29]. As such, the goal of this study was to demonstrate the successful implementation of this imaging methodology on a subset of ACRIN 6668 patients and to report statistics on the change in imaging parameters pre-RT and post-RT.

Materials and methods

Study cohort

This retrospective study, conducted at the Hospital of the University of Pennsylvania,

received Institutional Review Board approval and a Health Insurance Portability and Accountability Act (HIPAA) waiver. Patient data were obtained from the American College of Radiology Imaging Network (ACRIN) 6668/Radiation Therapy Oncology Group (RTOG) 0235, a prospective, multi-institutional trial investigating the potential prognostic role of FDG-PET imaging for patients with locally advanced NSCLC treated with definitive chemoradiotherapy (ClinicalTrials.gov identifier: NCT00083083). The study, described previously in detail [30], enrolled stage III and medically inoperable stage IIB NSCLC patients with no radiographic evidence of distant metastatic disease by conventional imaging and with Zubrod performance status [31] of 0-1, who received definitive platinum-based doublet chemotherapy concurrently with at least 50 Gy of thoracic radiation delivered in 1.8-2.0 Gy daily fractions.

FDG-PET/CT acquisition

All images were obtained according to the ACRIN 6668 protocol [30]. FDG-PET or FDG-PET/CT was performed on all patients prior to and approximately 14 weeks (12 to 16 weeks) following chemoradiotherapy on the same scanner qualified by the ACRIN Imaging Core Laboratory [32], with subsequent 2-year (or until death) follow-up as per standard clinical guidelines. All subjects fasted for at least 4 hours before receiving 0.14 to 0.21 mCi/kg (approximately 10 to 20 mCi) of FDG administered intravenously. Patients were required to have serum glucose levels of less than 200 mg/dL prior to radiotracer injection. Emission scanning began 50-70 minutes after FDG injection and included the body from the upper/mid neck to proximal femurs. Acquisition times for emission and transmission scans were in accordance with the manufacturer's recommendations. Patients consented to the original prospective study, which was approved by the local institutional review board of each participating institution.

Study population

In ACRIN 6668, a total of 181 patients completed both the pre-radiotherapy (pre-RT) and post-radiotherapy (post-RT) FDG-PET or FDG-PET/CT scans, of which 173 had all local read data supplied and were analyzed for the primary aim [30]. Images were collected centrally by ACRIN and transferred to the image-processing laboratory at the Hospital of the University of Pennsylvania for this secondary analysis. Given the exploratory nature of this analysis and limited available resources, a simple random sample of 40% (72/181) of patients was selected, with both pre-RT and post-RT FDG-PET/CT scans, for quantification of inflammation in both the ipsilateral and contralateral lung parenchyma. One patient was subsequently determined not to have received radiation therapy and so was excluded, arriving at the final analysis subset of 71 patients, with 142 individual lungs analyzed.

Quantitative image evaluation

The primary analysis of the FDG-PET/CT images was conducted individually using OsiriX MD software (Pixmeo SARL, Bernex, Switzerland). To obtain regions of interest (ROI) in the lung, transverse slices of the fused PET/CT images were manually contoured using a previously validated technique [33-35]. Images from the apex to the base of both the ipsilateral (same lung as the tumor location) and contralateral (opposite lung as the localization of tumor) lungs were used. Tumors within the lungs were included; however, all other surrounding structures, including mainstem bronchi, were excluded (**Figure 1**). Subsequently, the sectional lung mean standardized uptake value (sSUVmean) and sectional lung ROI area (sArea) were measured for each slice and exported for subsequent statistical analysis and comparative quantification.

Calculations of specific FDG-PET/CT quantitative parameters for the lung were performed according to methods described previously [34]. Preliminary calculations were conducted by summing all sectional lung volumes (sLV), the product of an individual slice ROI area (cm^2) and the slice thickness to yield total lung volumes for both pre-RT and post-RT scans. Sectional lung glycolysis (sLG), the product of sLV and sSUVmean per slice, was used to calculate global lung glycolysis (GLG). Lastly, lung SUVmean and global lung parenchymal glycolysis (GLPG) were calculated as shown in **Table 1**. All other equations of the

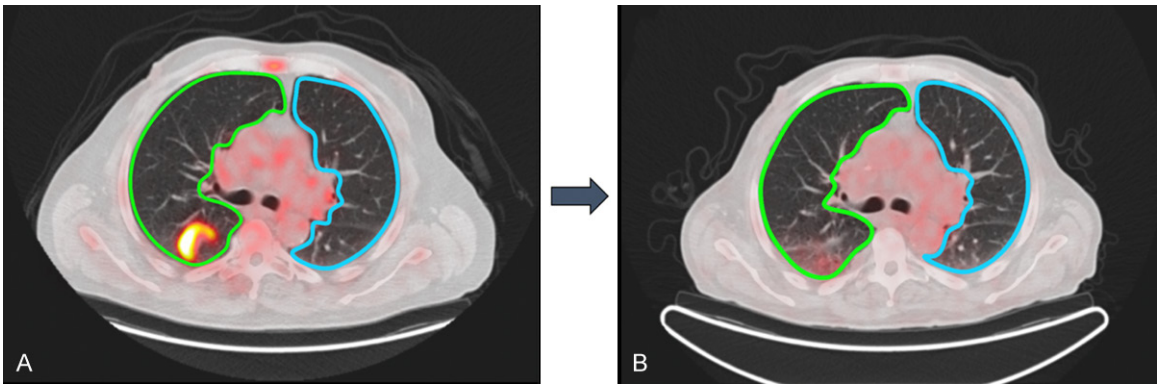

Figure 1. FDG-avid mass in the right lung due to lung cancer (A). The follow-up scan demonstrates that the tumor has responded to treatment (B). Regions of interest (ROI) were manually drawn on the fused PET/CT images, slice by slice axially from lung apex to base, for both the ipsilateral and contralateral lungs (green and blue outlines, respectively). Global lung glycolysis (GLG) was then calculated by adding all sectional lung glycolysis (sLG) from the lung.

Table 1. FDG-PET/CT parameter equations

FDG-PET/CT Parameters	Equation
Total LV	$\sum$ (*sSUVmean * sArea*)
GLG	$\sum$ (*sSUVmean * sLV*)
Lung SUVmean	*GLG/Total LV*
GLPG	GLG-TLG

Abbreviations: Total LV = total lung volume; GLG = global lung glycolysis; SUVmean = mean standardized uptake value; GLPG = global lung parenchymal glycolysis; sSUVmean = sectional lung mean standardized uptake value; sArea = sectional lung ROI area; sLV = sectional lung volume; TLG = total lesion glycolysis.

FDG-PET/CT parameters are demonstrated in **Table 1**.

In secondary calculations, tumor metabolic response to RT was quantified using metabolically active tumor volume (MTV), tumor SUV and TLG, as well as partial-volume-effect-corrected SUVmean (PVC-SUVmean) and TLG (PVC-TLG), of all FDG-avid lesions from the pre-RT FDG-PET/CT scans (**Figure 2**). To measure these values, a semiautomatic adaptive-contrast-oriented thresholding algorithm was implemented from a commercially available software package (ROVER software; ABX, Radeberg, Germany), which uses a predetermined background partial-volume-effect-correction and locally adaptive thresholding in an iterative algorithm model. The threshold was set at 40% of the maximum uptake within the mask [36]. A local background PVC algorithm was used to calculate partial volume correction (PVC). Finally, normal lung parenchymal inflammation as demonstrated on post-RT scans was calculated as below:

Δ Lung Parenchymal SUVmean = [(post RT GLG -post RT TLG)/(post RT LV-post RT MTV)]-[(pre RT GLG-pre RT TLG)/(pre RT LV-pre RT MTV)]

Δ Lung Parenchymal PVC SUVmean = [(post RT GLG-post RT PVC TLG)/(post RT LV-post RT MTV)]-[(pre RT GLG-pre RT PVC TLG)/(pre RT LV-pre RT MTV)]

Δ GLPG = (post RT GLG-post RT TLG)-(pre RT GLG-pre RT TLG)

Δ PVC GLPG = (post RT GLG-post RT PVC TLG)-(pre RT GLG-pre RT PVC TLG).

Statistical evaluation

The primary goal of this study was to implement FDG-PET/CT imaging as a tool for assessing chemoradiotherapy-induced lung inflammation and to compare the various FDG-PET/CT metrics from pre-RT to post-RT. An exploratory goal was to associate clinical characteristics with partial volume-corrected FDG-PET/CT parameters.

Descriptive statistics were calculated for each FDG-PET/CT parameter for both pre-RT and post-RT scans. The nonparametric Wilcoxon signed-rank test was used to compare paired pre-RT and post-RT measures for each FDG-PET/CT parameter. A Bonferroni correction was used to control the family-wise error rate among the 6 comparisons (ipsilateral lung: SUV, GLPG, PVC-SUV, PVC-GLPG; contralateral lung:

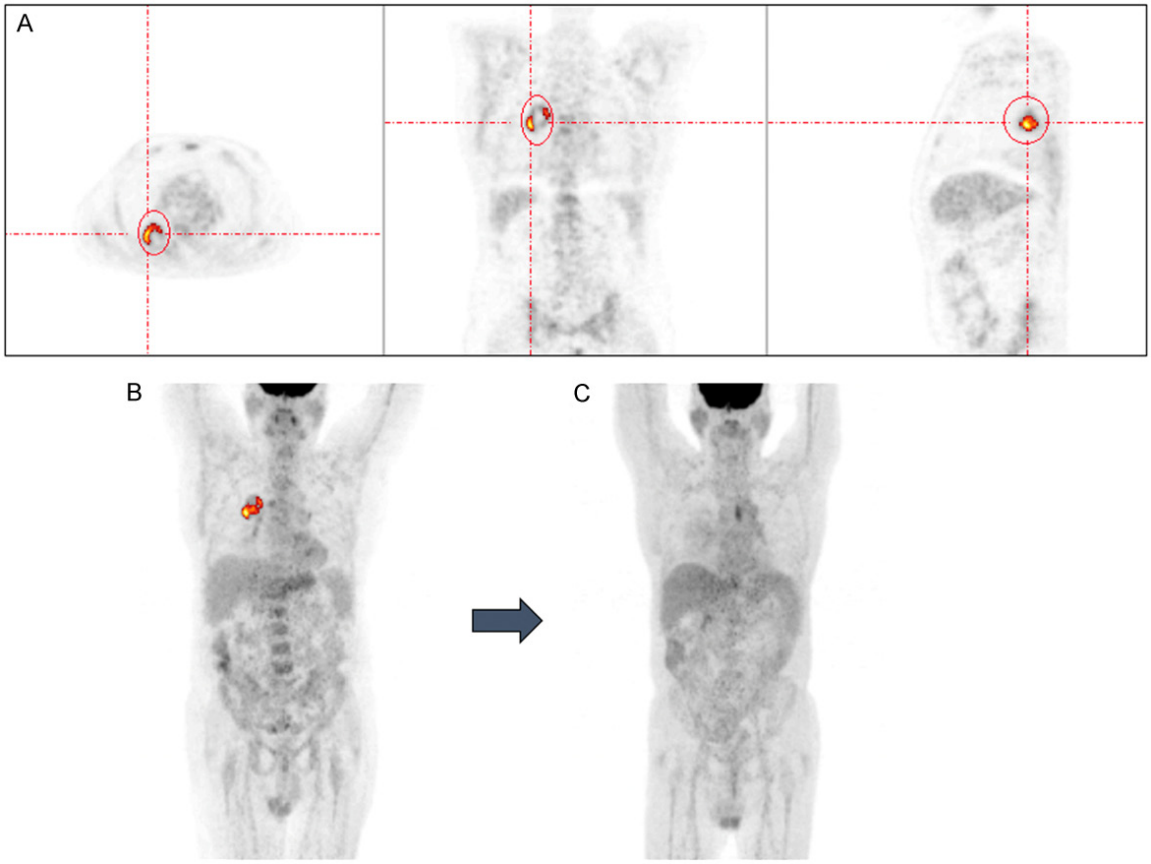

Figure 2. By placing masks on the FDG-avid lesions on all three planes (sagittal, coronal and axial) (A), the tumor regions (color overlay) are delineated (B) with the adaptive thresholding system of the ROVER software (ABX, Radeberg, Germany). Metabolic tumor volume (MTV) and Total lesion glycolysis (TLG) are automatically computed by the software, and TLG is then subtracted from GLG to calculate global lung parenchymal glycolysis (GLPG). The post-radiation therapy scan in the same patient (C).

SUV, GLPG), with significance threshold set to 0.05/6=0.008.

As an exploratory analysis, associations between partial volume corrected FDG-PET/CT parameters (with or without the natural logarithm transformation) in the ipsilateral lung and relevant clinical variables were assessed using univariate and multivariate linear models. The post-RT FDG-PET/CT measure was modeled on the basis of the corresponding pre-RT FDG-PET/CT measure and relevant clinical variables, also referred to as an ANCOVA model. Relevant clinical variables were assessed individually and then in a multivariate model, and included the following: age, gender, performance status (Fully active vs. Ambulatory, capable of light work), clinical-stage (IIB/IIIA vs. IIIB), radiation dose, and chemotherapy regimen (Carboplatin/Paclitaxel vs. Cisplatin/Etoposide vs. Other). As these modelling analyses were exploratory and viewed as hypothesis-generating, the models were not adjusted for multiplicity of inference. Data were analyzed using SAS version 9.4 software (SAS Institute, Cary, NC) and R version 3.4.4 software (R project; http://www.r-project.org/). All reported *P*-values are two-sided.

Results

Patient characteristics

A total of 71 patients were analyzed in the current study. Patient characteristics are shown in **Table 2**. There was a predominance of males (n=44, 62%), and the majority of patients were 60 years or older (median age=64). The most common tumor localization was reported in the upper lobes (n=39, 55%), followed by lower (n=21, 30%) and middle/lingula (n=7, 10%) lobes. The majority of patients were stage IIIA (n=44, 62%) or IIIB (n=23, 32%). Patients received definitive platinum-based doublet chemotherapy concurrently with at least 50 Gy

Table 2. Demographic and clinical characteristics

Demographic or Clinical Characteristic	ACRIN 6668: Patients with both pre- and post-RT PET/CT (N=181)		Analysis set (N=71)	
	N	%	N	%
Age, years				
Mean (std dev)	64.4 (9.4)		62.5 (8.8)	
Median (range)	65 (36, 84)		64 (37, 78)	
Sex				
Male	118	65%	44	62%
Female	63	35%	27	38%
Race[1]				
White	142	78%	56	79%
African American	15	8%	6	8%
Asian	22	12%	7	10%
Other/Unknown	5	3%	3	4%
Ethnicity				
Hispanic or Latino	5	3%	3	4%
Not Hispanic or Latino	171	94%	67	94%
Unknown	5	3%	1	1%
Clinical stage				
IIB	7	4%	4	6%
IIIA	101	56%	44	62%
IIIB	73	40%	23	32%
Location of primary tumor				
RUL	59	33%	22	31%
RLL	35	19%	16	23%
R hilum/middle lobe	16	9%	7	10%
LUL	46	25%	17	24%
LLL	14	8%	5	7%
Multiple lobes-right lung	10	6%	4	6%
Multiple lobes-left lung	1	<1%	0	0%
Performance status				
Fully active	88	49%	42	59%
Ambulatory, capable of light work	93	51%	29	41%
Chemotherapy regimen				
Carboplatin/Paclitaxel	78	43%	30	42%
Cisplatin/Etoposide	30	17%	10	14%
Other	73	40%	31	44%
Radiation dose				
Data not available	2	1%	0	0%
50-60 Gy	8	4%	4	6%
60-70 Gy	129	71%	50	70%
≥70 Gy	42	23%	17	24%

Abbreviations: RUL = right upper lobe; RLL = right lower lobe; LUL = left upper lobe; LLL = left lower lobe. [1]Multiple races could be endorsed by the same patient, such that the total over all options may sum to greater than 100%.

of thoracic radiation delivered in 1.8-2.0 Gy daily fractions. The majority of patients received 60-70 Gy (n=50, 70%), while a smaller number received 50-60 Gy (n=4, 6%) or 70 Gy or greater (n=17, 24%). Regarding the chemotherapy regimens, patients received either Carboplatin/

Table 3. Summary statistics of FDG-PET/CT parameters (Pre- and Post-RT)

			Mean (SD)	Median	Min	Max	*P*-value[1]
Ipsilateral lung	SUVmean	Pre-RT	0.70 (0.30)	0.65	0.22	1.76	**<0.0001**
		Post-RT	0.98 (0.44)	0.89	0.35	2.35	
	GLPG	Pre-RT	1763.27 (1004.31)	1545.15	337.21	5741.93	**0.004**
		Post-RT	2116.17 (1199.55)	1864.50	138.19	5011.57	
	PVC-SUVmean	Pre-RT	0.66 (0.31)	0.60	0.17	1.90	**<0.0001**
		Post-RT	0.98 (0.44)	0.89	0.35	2.35	
	PVC-GLPG	Pre-RT	1652.83 (952.94)	1475.90	129.31	5579.83	**<0.0001**
		Post-RT	2116.17 (1199.55)	1864.50	138.19	5011.57	
Contralateral lung	SUVmean	Pre-RT	0.57 (0.15)	0.56	0.25	0.94	0.18
		Post-RT	0.60 (0.17)	0.58	0.31	1.28	
	GLPG	Pre-RT	1356.26 (570.74)	1225.20	493.14	3012.16	0.12
		Post-RT	1488.77 (726.63)	1328.29	565.71	4755.69	

Abbreviations: SUV = standardized uptake value; GLPG = global lung parenchymal glycolysis; PVC = partial volume correction; RT = radiation therapy. [1]*P*-value corresponding to the comparison of the pre-RT versus the corresponding post-RT is based on the nonparametric Wilcoxon signed rank test. *P*-values below the multiplicity-corrected threshold of 0.05/6=0.008 are shown in bold.

Paclitaxel (n=30, 42%), Cisplatin/Etoposide (n=10, 14%) or other types of chemotherapy treatments (n=31, 44%).

Change in FDG-PET/CT parameters

Descriptive statistics of FDG-PET parameters by time point in both the ipsilateral and contralateral lung are shown in **Table 3**. In the ipsilateral lung, across all patients, there was a significant increase in both SUVmean (relative change 40%) and GLPG (relative change 20%) between the pre-RT and post-RT FDG-PET/CT scans (P<0.0001 and P=0.004, respectively) (**Table 3**). The absolute increases in PVC-SUVmean and PVC-GLPG were higher than their uncorrected counterparts (ΔPVC-SUVmean 0.32 versus ΔSUVmean 0.28; ΔPVC-GLPG 463.34 cc versus ΔGLPG 352.90 cc), and both were highly significant (P<0.0001; **Figure 3**). In the contralateral lung, across all patients, there was no significant difference in either SUVmean or GLPG between the pre-RT and post-RT FDG-PET/CT scans (P=0.18 and P=0.12, respectively).

Association of FDG-PET/CT parameters with clinical features

In exploratory analyses, we associated FDG-PET/CT measurements in the ipsilateral lung with pre-specified clinical characteristics. In particular, linear models were fit, regressing the post-RT measure against the corresponding pre-RT measure and clinical variables. For PVC-SUVmean, when examining clinical variables individually, the only clinical feature significantly associated with post-RT PVC-SUVmean, adjusting for the corresponding pre-RT value, was the clinical stage (results not shown). This association remained after adjusting for the other pre-specified clinical features, where the adjusted estimate suggests that stage IIB/IIIA patients on average exhibit a post-RT PVC-SUVmean that is 0.22 units higher than stage IIIB patients (95% CI: 0.02-0.41; P=0.03); however, the R2 value for the model was low (R^2= 0.35), suggesting that pre-RT PVC-SUVmean and the included clinical features account for only 35% of the observed variation in post-RT PVC-SUVmean. The multivariate model is shown in **Table 4**. This association remained when the small number of patients with stage IIB in the analysis set (n=4) were excluded [multivariate estimate=0.24, 95% CI: 0.04-0.44; P=0.02].

For PVC-GLPG, when examining clinical variables individually, the only clinical feature significantly associated with post-RT PVC-GLPG, adjusting for the corresponding pre-RT value, was again the clinical stage (results not shown). This association remained after adjusting for the other clinical features, where the adjusted estimate suggests that stage IIB/IIIA patients on average exhibit a post-RT GLPG that is 1.57-fold higher than stage IIIB patients (95% CI: 1.23-2.01; P=0.0005). The multivariate model is shown in **Table 5**, which exhibited only a mod-

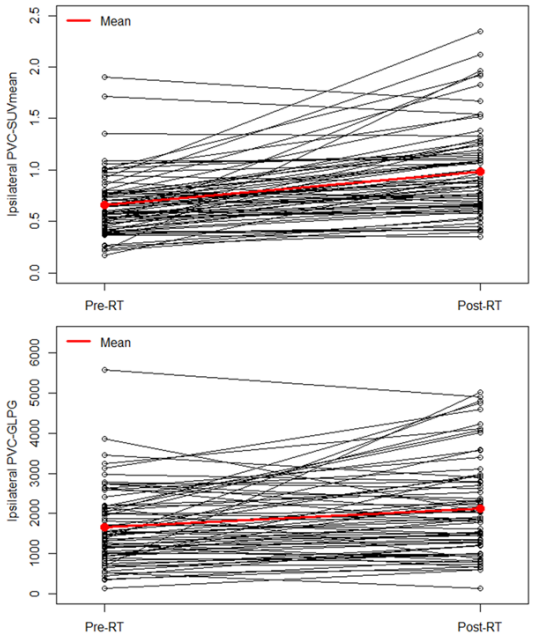

Figure 3. Change in PVC-SUVmean and PVC-GLPG of the ipsilateral lung from pre- to post-RT.

est R^2 value (R^2=0.51). Again, this association remained when the small number of patients with stage IIB in the analysis set (n=4) were excluded [1.57-fold increase, 95% CI: 1.22-2.03; P=0.0007].

Discussion

The current study demonstrated induction of an inflammatory response in the ipsilateral lung of NSCLC patients treated with photon RT, suggesting that the FDG-PET/CT parameters of SUVmean and global lung parenchymal glycolysis may serve as biomarkers for the prediction of radiation pneumonitis (RP) status.

RP is one of the most serious complications of chest RT, as it impairs respiratory function and decreases quality of life [37]. Clinical diagnosis of RP relies on the assessment of respiratory symptoms, radiographic changes, and timing of the administered RT. However, the incidence of RP ranges between 15% and 58%, largely due to variations in evaluation methods, symptom assessment, and clinical practice [22, 38, 39]. Furthermore, the variety of metabolically active confounders that exist in patients with NSCLC, including residual malignancy, drug-induced pneumonitis, acute infection, esophagitis or pericarditis, and pulmonary edema, has made the diagnosis of RP a major clinical challenge. In one study of 318 lung cancer patients who underwent chemoradiotherapy, diagnosis with at least Grade 2 RP was found to be due to factors unrelated to therapy in 13 (28%) of the 47 diagnosed patients [40]. Similarly, Yirmibesoglu et al. reported that 48% of NSCLC patients diagnosed with clinical RP post-RT had potential confounding characteristics, such as concomitant infection, chronic obstructive pulmonary disease, cardiac disease, and tumor regrowth [41]. Thus, more refined methods to predict and identify chest RT patients with RP remains a significant clinical unmet need, which is why demonstrating successful implementation of FDG-PET/CT imaging in this particular cohort is so important.

This study measured changes in FDG uptake in the lung parenchyma on FDG-PET/CT images pre- and post-RT to quantify lung inflammatory response in patients with locally advanced NSCLC receiving photon RT. In a previous retrospective pilot study, our group used FDG-PET/CT to quantify global lung inflammation following lung RT, reporting significant increases in lung parenchyma SUVmean and GLPG post-RT in the ipsilateral lung [33]. Our results here, obtained from a larger-scale prospective study population, corroborate these findings, showing significant increases in the average SUVmean and GLPG of the ipsilateral but not the contralateral lung when comparing pre- and post-RT images. This study, therefore, lends further support to the hypothesis that FDG-PET/CT may be an effective imaging modality to detect and quantify inflammatory responses to therapy in lung cancer patients who receive chest RT.

Previous investigations of the use of FDG-PET/CT for the detection of RP in lung cancer patients have shown promising results [42-46], despite varying methodologies and a number of limitations. Several studies have described the implementation of visual scoring systems in which a nuclear medicine physician assigns radiotoxicity scores to FDG-PET/CT scans post-RT. While such studies report a significant correlation between assigned scores and the presence of clinical respiratory symptoms [42, 43, 47], they rely on subjective image interpretation and semi-quantitative parameters, factors that are limited by physician expertise and

Table 4. Association of post-RT PVC-SUVmean in the ipsilateral lung with the corresponding pre-RT value and relevant clinical features through an ANCOVA linear model

	Estimate (SE)	*P*-value
Intercept	0.86 (0.14)	<0.0001
Pre-RT PVC-SUVmean[1,2]	0.72 (0.15)	<0.0001
Age[1,3]	0.001 (0.03)	0.97
Total radiation dose[1,4]	-0.08 (0.05)	0.14
Sex: Male (vs. Female)	-0.08 (0.10)	0.41
Performance status: Fully active (vs. Ambulatory capable of light work)	-0.05 (0.09)	0.57
Clinical stage: IIB/IIIA (vs. IIIB)	0.22 (0.10)	0.03
Chemotherapy regimen: Carboplatin + Paclitaxel (vs. Other)	0.08 (0.10)	0.41
Chemotherapy regimen: Cisplatin + Etoposide (vs. Other)	0.18 (0.15)	0.21
R^2=0.35		

Abbreviations: SUV = standardized uptake value; PVC = partial volume correction; RT = radiation therapy; SE = standard error. [1]Continuous covariates were centered at the corresponding mean value. [2]The estimate for pre-RT PVC-SUVmean is interpreted per 1-unit increase. [3]The estimate for Age is interpreted per 5-year increase in age. [4]The estimate for Total Radiation dose is interpreted per 5-Gy increase in dose.

Table 5. Association of post-RT PVC-GLPG in the ipsilateral lung (on the natural log scale) with the corresponding pre-RT value and relevant clinical features through an ANCOVA linear model

	Estimate (SE)[1]	*P*-value
Intercept	7.17 (0.17)	<0.0001
Pre-RT GLG[2,3]	0.04 (0.01)	<0.0001
Age[2,4]	0.02 (0.04)	0.52
Total radiation dose[2,5]	-0.07 (0.07)	0.31
Sex: Male (vs. Female)	0.06 (0.12)	0.65
Performance status: Fully active (vs. Ambulatory capable of light work)	-0.07 (0.12)	0.51
Clinical stage: IIB/IIIA (vs. IIIB)	0.45 (0.12)	0.0005
Chemotherapy regimen: Carboplatin + Paclitaxel (vs. Other)	-0.02 (0.13)	0.88
Chemotherapy regimen: Cisplatin + Etoposide (vs. Other)	0.18 (0.18)	0.34
R^2=0.51		

Abbreviations: GLPG = global lung parencyma glycolysis; PVC = partial volume correction; RT = radiation therapy; SE = standard error. [1]Post-RT PVC-GLPG was modeled on the natural log scale to control for heteroscedasticity. Parameter estimates then represent the multiplicative increase in the Post-RT PVC-GLPG. For example, adjusting for other covariates, on average the post-RT PVC-GLPG value for stage IIB/IIIA patients is $e^{0.45}$=1.57 times greater than that of stage IIIB patients. [2]Continuous covariates were centered at the corresponding mean value. [3]The estimate for pre-RT PVC-GLG is interpreted per 100-unit increase. [4]The estimate for Age is interpreted per 5-year increase in age. [5]The estimate for Total Radiation dose is interpreted per 5-Gy increase in dose.

metabolically active confounders, respectively. In a more recent study, Guerrero et al. proposed a pulmonary metabolic radiation response (PMRR) parameter, calculated as the slope of FDG uptake in lung tissue normalized to that in the non-irradiated lung versus the radiation dose, and they found a significant correlation between PMRR and both RP risk and RP clinical scores in patients who underwent chest RT [21, 29]. While promising, widespread implementation of such an approach would likely be challenging, as it would require detailed quantitative information from RT treatment plans and post-RT FDG-PET/CT images, which are often not available in non-academic settings.

Our approach to the quantification of post-RT lung inflammation may offer a more objective technique as an imaging biomarker in future prospective study to predict true clinical RP status. A notable component of our approach is the consideration of PVC in GLG and GLPG calculations. The partial volume effect, a result of the limited spatial resolution of PET scanners, image sampling effects, and organ motion during image acquisition, has been shown to be a

significant limitation of SUV measurements in quantification by PET [48, 49]. Our original pilot study demonstrated the importance of employing PVC, as PVC measurements all showed larger differences in FDG-PET/CT parameters compared to the uncorrected measurements [33], and previous work has similarly demonstrated the value of PVC in avoiding underestimation of lung inflammation [49, 50]. Our current results provide further evidence for the need to consider PVC in quantifying post-RT lung inflammation, as again absolute increases in PVC-SUVmean and PVC-GLPG were more obvious than in their uncorrected counterparts (ΔPVC-SUVmean 0.32 versus ΔSUVmean 0.28; ΔPVC-GLPG 463.34 cc versus ΔGLPG 352.90 cc).

There are several studies that have reported associations between different clinical features and the risk of RP with partially different results [20-25], and there is currently no established method to predict RP [21]. The only clinical variable significantly associated with the FDG-PET/CT parameters in our study was the clinical tumor stage. This association remained when adjusting for other clinical variables. Stage IIIB includes primary tumor classification (T-classification) T1a-T2b with bilateral lymph node affection and T3/T4 with ipsilateral lymph node affection. In patients with Stage IIIB tumors and T1a-T2b classification, the primary lung tumor could be relatively small relative to IIB and IIIA patients with higher T-classification. This could possibly explain the lower post-treatment values observed in the ipsilateral lung compared to stage IIB and IIIA.

Our study has several limitations. For instance, our method of lung segmentation is very time consuming and may be difficult to translate to widespread routine use without the development of automated, computer-assisted techniques. As a result, we only analyzed a 40% random sample of the available ACRIN 6668 cases. There is to our knowledge no currently available commercial product to accomplish this task. However, with the development of more advanced software, it might be feasible to automate such methods to quantify lung diseases including lung inflammation automatically or semi-automatically in the future. Additionally, this study did not make use of clinical scoring systems to correlate or compare FDG-PET/CT inflammatory quantification and patient symptoms such as low fever, short breath, and cough, as these data were not collected in the original ACRIN 6668 trial. Furthermore, the ACRIN 6668 trial did not register information on corticosteroid therapy allowing for subset analysis. It is important to note that FDG administration requires patients to adhere to a special diet, including six hours of fasting prior to the scan, which is not necessary for other more widely used imaging modalities. However, the addition of functional assessment to anatomic scans is indispensable in disorders that exhibit early transient progression, such as RP, which makes FDG-PET/CT an ideal choice in evaluating this pathology.

Although corticosteroids are the cornerstone of clinical management of RP, advanced knowledge of molecular mechanisms underlying lung injury has led to the development of other promising pharmaceuticals to treat this disease [18]. This is clinically significant, since long-term corticosteroid use can have detrimental side effects, including osteoporosis, Cushing's syndrome, infections, edema, and early cataract development. Evaluating patients' responsiveness to these newly elucidated therapeutics is key in determining their effectiveness and safety in treating RP. Therefore, a molecular imaging technique with quantification will be of even more importance for the detection, selection, and follow-up of patients with RP in the future.

Conclusion

In conclusion, our study demonstrates the value of FDG-PET/CT in the quantification of lung inflammation post-RT in patients with lung cancer treated with definitive chemoradiation. Through the use of volume-based and quantitative PET parameters, GLPG and lung parenchymal SUVmean, significant changes were found pre-RT to post-RT in the ipsilateral but not contralateral lung, suggesting that these values may have the potential to serve as sensitive imaging biomarkers for RP detection. Further evaluation in large-scale trials with rigorous clinical assessment of RP is warranted to validate that this imaging technique can accurately predict clinical RP status.

Acknowledgements

This study was coordinated by the ECOG-ACRIN Cancer Research Group (Peter J. O'Dwyer, MD

and Mitchell D. Schnall, MD, PhD, Group Co-Chairs) and supported by the National Cancer Institute of the National Institutes of Health under the following award numbers: U10CA180820, U10CA180794. The content is solely the responsibility of the authors and does not necessarily represent the official views of the National Institutes of Health, nor does mention of trade names, commercial products, or organizations imply endorsement by the U.S. government.

Disclosure of conflict of interest

None.

Abbreviations

NSCLC, non-small cell lung cancer; RT, radiation therapy; PET, positron emission tomography; MRI, magnetic resonance imaging; FDG, 18F-2-fluoro-2-deoxy-D-glucose; CCRT, concurrent chemoradiotherapy; ROI, regions of interest; SUVmean, mean standardized uptake value; PVC, partial volume correction; GLG, global lung glycolysis; GLPG, global lung parenchymal glycolysis.

Address correspondence to: Abass Alavi, Department of Radiology, Hospital of The University of Pennsylvania, 3400 Spruce Street, Philadelphia 19104, PA, USA. Tel: 215-662-3069; Fax: 215-573-4107; E-mail: abass.alavi@pennmedicine.upenn.edu

References

[1] USCS Data Visualizations n.d. https://gis.cdc.gov/grasp/USCS/DataViz.html (accessed May 24, 2020).

[2] Duma N, Santana-Davila R and Molina JR. Non-small cell lung cancer: epidemiology, screening, diagnosis, and treatment. Mayo Clin Proc 2019; 94: 1623-40.

[3] Siegel RL, Miller KD and Jemal A. Cancer statistics, 2019. CA Cancer J Clin 2019; 69: 7-34.

[4] Goldstraw P, Chansky K, Crowley J, Rami-Porta R, Asamura H, Eberhardt WE, Nicholson AG, Groome P, Mitchell A and Bolejack V; International Association for the Study of Lung Cancer Staging and Prognostic Factors Committee, Advisory Boards, and Participating Institutions; International Association for the Study of Lung Cancer Staging and Prognostic Factors Committee Advisory Boards and Participating Institutions. The IASLC lung cancer staging project: proposals for revision of the TNM stage groupings in the forthcoming (Eighth) edition of the TNM classification for lung cancer. J Thorac Oncol 2016; 11: 39-51.

[5] Bentzen SM. Preventing or reducing late side effects of radiation therapy: radiobiology meets molecular pathology. Nat Rev Cancer 2006; 6: 702-13.

[6] Arrieta O, Gallardo-Rincón D, Villarreal-Garza C, Michel RM, Astorga-Ramos AM, Martínez-Barrera L and de la Garza J. High frequency of radiation pneumonitis in patients with locally advanced non-small cell lung cancer treated with concurrent radiotherapy and gemcitabine after induction with gemcitabine and carboplatin. J Thorac Oncol 2009; 4: 845-52.

[7] Borja AJ, Hancin EC, Dreyfuss AD, Zhang V, Mathew T, Rojulpote C, Werner TJ, Patil S, Gonuguntla K, Lin A, Feigenberg SJ, Swisher-McClure S, Alavi A and Revheim ME. 18F-FDG-PET/CT in the quantification of photon radiation therapy-induced vasculitis. Am J Nucl Med Mol Imaging 2020; 10: 66-73.

[8] Hancin E, Borja A, Mouminah A, Taghvaei R, Koa B, Rojulpote KV, Werner T, Revheim ME and Alavi A. Role of FDG in the management of radiation-induced complications in patients with head and neck malignancies. J Nucl Med 2020; 61: 1185

[9] Kong FM, Ten Haken R, Eisbruch A and Lawrence TS. Non-small cell lung cancer therapy-related pulmonary toxicity: an update on radiation pneumonitis and fibrosis. Semin Oncol 2005; 32 Suppl 3: S42-54.

[10] Verma V, Simone CB and Werner-Wasik M. Acute and late toxicities of concurrent chemoradiotherapy for locally-advanced non-small cell lung cancer. Cancers (Basel) 2017; 9: 120.

[11] Bradley JD, Hope A, El Naqa I, Apte A, Lindsay PE, Bosch W, Matthews J, Sause W, Graham MV and Deasy JO; RTOG. A nomogram to predict radiation pneumonitis, derived from a combined analysis of RTOG 9311 and institutional data. Int J Radiat Oncol Biol Phys 2007; 69: 985-92.

[12] Weller A, O'Brien MER, Ahmed M, Popat S, Bhosle J, McDonald F, Yap T, Du Y, Vlahos I and deSouza NM. Mechanism and non-mechanism based imaging biomarkers for assessing biological response to treatment in non-small cell lung cancer. Eur J Cancer 2016; 59: 65-78.

[13] Zhang XJ, Sun JG, Sun J, Ming H, Wang XX, Wu L and Chen ZT. Prediction of radiation pneumonitis in lung cancer patients: a systematic review. J Cancer Res Clin Oncol 2012; 138: 2103-16.

[14] Rodrigues G, Lock M, D'Souza D, Yu E and Van Dyk J. Prediction of radiation pneumonitis by dose-volume histogram parameters in lung

cancer--a systematic review. Radiother Oncol 2004; 71: 127-38.
[15] Wahl RL, Jacene H, Kasamon Y and Lodge MA. From RECIST to PERCIST: evolving considerations for PET response criteria in solid tumors. J Nucl Med 2009; 50 Suppl 1: 122S-50S.
[16] Novello S, Giaj Levra M and Vavalà T. Functional imaging in predicting response to antineoplastic agents and molecular targeted therapies in lung cancer: a review of existing evidence. Crit Rev Oncol Hematol 2012; 83: 208-15.
[17] Abratt RP, Morgan GW, Silvestri G and Willcox P. Pulmonary complications of radiation therapy. Clin Chest Med 2004; 25: 167-77.
[18] Bledsoe TJ, Nath SK and Decker RH. Radiation pneumonitis. Clin Chest Med 2017; 38: 201-8.
[19] Borst GR, De Jaeger K, Belderbos JS, Burgers SA and Lebesque JV. Pulmonary function changes after radiotherapy in non-small-cell lung cancer patients with long-term disease-free survival. Int J Radiat Oncol Biol Phys 2005; 62: 639-44.
[20] Anthony GJ, Cunliffe A, Castillo R, Pham N, Guerrero T, Armato SG 3rd and Al-Hallaq HA. Incorporation of pre-therapy 18 F-FDG uptake data with CT texture features into a radiomics model for radiation pneumonitis diagnosis. Med Phys 2017; 44: 3686-94.
[21] Hart JP, McCurdy MR, Ezhil M, Wei W, Khan M, Luo D, Munden RF, Johnson VE and Guerrero TM. Radiation pneumonitis: correlation of toxicity with pulmonary metabolic radiation response. Int J Radiat Oncol Biol Phys 2008; 71: 967-71.
[22] Palma DA, Senan S, Tsujino K, Barriger RB, Rengan R, Moreno M, Bradley JD, Kim TH, Ramella S, Marks LB, De Petris L, Stitt L and Rodrigues G. Predicting radiation pneumonitis after chemoradiation therapy for lung cancer: an international individual patient data meta-analysis. Int J Radiat Oncol Biol Phys 2013; 85: 444-50.
[23] Jin H, Tucker SL, Liu HH, Wei X, Yom SS, Wang S, Komaki R, Chen Y, Martel MK, Mohan R, Cox JD and Liao Z. Dose-volume thresholds and smoking status for the risk of treatment-related pneumonitis in inoperable non-small cell lung cancer treated with definitive radiotherapy. Radiother Oncol 2009; 91: 427-32.
[24] Robnett TJ, Machtay M, Vines EF, McKenna MG, Algazy KM and McKenna WG. Factors predicting severe radiation pneumonitis in patients receiving definitive chemoradiation for lung cancer. Int J Radiat Oncol Biol Phys 2000; 48: 89-94.
[25] Wen J, Liu H, Wang Q, Liu Z, Li Y, Xiong H, Xu T, Li P, Wang LE, Gomez DR, Mohan R, Komaki R, Liao Z and Wei Q. Genetic variants of the LIN28B gene predict severe radiation pneumonitis in patients with non-small cell lung cancer treated with definitive radiation therapy. Eur J Cancer 2014; 50: 1706-16.
[26] Houshmand S, Boursi B, Salavati A, Simone CB and Alavi A. Applications of fluorodeoxyglucose PET/computed tomography in the assessment and prediction of radiation therapy-related complications. PET Clin 2015; 10: 555-71.
[27] Kong FM and Wang S. Nondosimetric risk factors for radiation-induced lung toxicity. Semin Radiat Oncol 2015; 25: 100-9.
[28] Echeverria AE, McCurdy M, Castillo R, Bernard V, Ramos NV, Buckley W, Castillo E, Liu P, Martinez J and Guerrero T. Proton therapy radiation pneumonitis local dose-response in esophagus cancer patients. Radiother Oncol 2013; 106: 124-9.
[29] Guerrero T, Johnson V, Hart J, Pan T, Khan M, Luo D, Liao Z, Ajani J, Stevens C and Komaki R. Radiation pneumonitis: local dose versus [18F]-fluorodeoxyglucose uptake response in irradiated lung. Int J Radiat Oncol Biol Phys 2007; 68: 1030-5.
[30] Machtay M, Duan F, Siegel BA, Snyder BS, Gorelick JJ, Reddin JS, Munden R, Johnson DW, Wilf LH, DeNittis A, Sherwin N, Cho KH, Kim SK, Videtic G, Neumann DR, Komaki R, Macapinlac H, Bradley JD and Alavi A. Prediction of survival by [18F]fluorodeoxyglucose positron emission tomography in patients with locally advanced non-small-cell lung cancer undergoing definitive chemoradiation therapy: results of the ACRIN 6668/RTOG 0235 trial. J Clin Oncol 2013; 31: 3823-30.
[31] West HJ and Jin JO. JAMA oncology patient page. Performance status in patients with cancer. JAMA Oncol 2015; 1: 998.
[32] Scheuermann JS, Saffer JR, Karp JS, Levering AM and Siegel BA. Qualification of PET scanners for use in multicenter cancer clinical trials: the american college of radiology imaging network experience. J Nucl Med 2009; 50: 1187-93.
[33] Abdulla S, Salavati A, Saboury B, Basu S, Torigian DA and Alavi A. Quantitative assessment of global lung inflammation following radiation therapy using FDG PET/CT: a pilot study. Eur J Nucl Med Mol Imaging 2014; 41: 350-6.
[34] Jahangiri P, Pournazari K, Torigian DA, Werner TJ, Swisher-McClure S, Simone CB 2nd and Alavi A. A prospective study of the feasibility of FDG-PET/CT imaging to quantify radiation-induced lung inflammation in locally advanced non-small cell lung cancer patients receiving proton or photon radiotherapy. Eur J Nucl Med Mol Imaging 2019; 46: 206-16.
[35] Rice SR, Saboury B, Houshmand S, Salavati A, Kalbasi A, Goodman CR, Werner TJ, Vujaskovic

Z, Simone CB 2nd and Alavi A. Quantification of global lung inflammation using volumetric 18F-FDG PET/CT parameters in locally advanced non-small-cell lung cancer patients treated with concurrent chemoradiotherapy: a comparison of photon and proton radiation therapy. Nucl Med Commun 2019; 40: 618-25.

[36] Aide N, Lasnon C, Veit-Haibach P, Sera T, Sattler B and Boellaard R. EANM/EARL harmonization strategies in PET quantification: from daily practice to multicentre oncological studies. Eur J Nucl Med Mol Imaging 2017; 44 Suppl 1: 17-31.

[37] Torre-Bouscoulet L, Muñoz-Montaño WR, Martínez-Briseño D, Lozano-Ruiz FJ, Fernández-Plata R, Beck-Magaña JA, García-Sancho C, Guzmán-Barragán A, Vergara E, Blake-Cerda M, Gochicoa-Rangel L, Maldonado F, Arroyo-Hernández M and Arrieta O. Abnormal pulmonary function tests predict the development of radiation-induced pneumonitis in advanced non-small cell lung Cancer. Respir Res 2018; 19: 72.

[38] Parashar B, Edwards A, Mehta R, Pasmantier M, Wernicke AG, Sabbas A, Kerestez RS, Nori D and Chao KS. Chemotherapy significantly increases the risk of radiation pneumonitis in radiation therapy of advanced lung cancer. Am J Clin Oncol 2011; 34: 160-4

[39] Salinas FV and Winterbauer RH. Radiation pneumonitis: a mimic of infectious pneumonitis. Semin Respir Infect 1995; 10: 143-53.

[40] Kocak Z, Evans ES, Zhou SM, Miller KL, Folz RJ, Shafman TD and Marks LB. Challenges in defining radiation pneumonitis in patients with lung cancer. Int J Radiat Oncol Biol Phys 2005; 62: 635-8.

[41] Yirmibesoglu E, Higginson DS, Fayda M, Rivera MP, Halle J, Rosenman J, Xie L and Marks LB. Challenges scoring radiation pneumonitis in patients irradiated for lung cancer. Lung Cancer Amst Neth 2012; 76: 350-3.

[42] Hicks RJ, Mac Manus MP, Matthews JP, Hogg A, Binns D, Rischin D, Ball DL and Peters LJ. Early FDG-PET imaging after radical radiotherapy for non-small-cell lung cancer: inflammatory changes in normal tissues correlate with tumor response and do not confound therapeutic response evaluation. Int J Radiat Oncol Biol Phys 2004; 60: 412-8.

[43] Mac Manus MP, Ding Z, Hogg A, Herschtal A, Binns D, Ball DL and Hicks RJ. Association between pulmonary uptake of fluorodeoxyglucose detected by positron emission tomography scanning after radiation therapy for non-small-cell lung cancer and radiation pneumonitis. Int J Radiat Oncol Biol Phys 2011; 80: 1365-71.

[44] McCurdy MR, Castillo R, Martinez J, Al Hallack MN, Lichter J, Zouain N and Guerrero T. [18F]-FDG uptake dose-response correlates with radiation pneumonitis in lung cancer patients. Radiother Oncol 2012; 104: 52-7.

[45] Petit SF, van Elmpt WJ, Oberije CJ, Vegt E, Dingemans AM, Lambin P, Dekker AL and De Ruysscher D. [18F]fluorodeoxyglucose uptake patterns in lung before radiotherapy identify areas more susceptible to radiation-induced lung toxicity in non-small-cell lung cancer patients. Int J Radiat Oncol Biol Phys 2011; 81: 698-705.

[46] Teo BK, Abelson J, Teo A, Graves EE, Guerrero T and Loo BW. Time interval to FDG PET/CT after mediastinal radiation impacts the dose response of pneumonitis related metabolic activity. Int J Radiat Oncol Biol Phys 2008; 72: S67-8.

[47] Kong FM, Frey KA, Quint LE, Ten Haken RK, Hayman JA, Kessler M, Chetty IJ, Normolle D, Eisbruch A and Lawrence TS. A pilot study of [18F]fluorodeoxyglucose positron emission tomography scans during and after radiation-based therapy in patients with non small-cell lung cancer. J Clin Oncol 2007; 25: 3116-23.

[48] Basu S, Zaidi H, Houseni M, Bural G, Udupa J, Acton P, Torigian DA and Alavi A. Novel quantitative techniques for assessing regional and global function and structure based on modern imaging modalities: implications for normal variation, aging and diseased states. Semin Nucl Med 2007; 37: 223-39.

[49] Soret M, Bacharach SL and Buvat I. Partial-volume effect in PET tumor imaging. J Nucl Med 2007; 48: 932-45.

[50] Hofheinz F, Dittrich S, Pötzsch C and Hoff Jv. Effects of cold sphere walls in PET phantom measurements on the volume reproducing threshold. Phys Med Biol 2010; 55: 1099-113.